aerospace

MDPI

Article

Assignment of Natural Frequencies and Mode Shapes Based on FRFs

Jun Ren * and **Qiuyu Cao**

School of Mechanical Engineering, Hubei University of Technology, Wuhan 430068, China; caoqiuyu20210517@163.com

* Correspondence: renjun@mail.hbut.edu.cn

Abstract: This paper proposes a method of structural modification for the assignment of natural frequencies and mode shapes based on frequency response functions (FRFs). The method involves the addition of masses or stiffness (supporting stiffness or connection stiffness), the simultaneous addition of masses and stiffness, or the addition of mass-spring substructures to the original structure. Firstly, the proposed technique was formulated as an optimization problem based on the FRFs of the original structure and the masses or stiffness that needed to be added. Next, the required added masses and stiffness were obtained by solving the optimization problem using a genetic algorithm. Finally, numerical verification was performed for the different structural modification schemes. The results show that, compared to only adding either stiffness or masses, adding both simultaneously or adding spring-mass substructures obtained better optimization results. The advantage of this FRFs-based method is that the FRFs can be directly measured by modal testing, without knowledge of analytical or modal models. Furthermore, multiple structural modifications were considered in the assignment of natural frequencies and mode shapes, making the application of this method more applicable to engineering.

Keywords: frequency response functions (FRFs); assignment of natural frequencies and modes; structural modification; genetic algorithm

Citation: Ren, J.; Cao, Q. Assignment of Natural Frequencies and Mode Shapes Based on FRFs. *Aerospace* **2021**, *8*, 262. https://doi.org/10.3390/aerospace8090262

Academic Editor: Rosario Pecora

Received: 29 June 2021
Accepted: 9 September 2021
Published: 14 September 2021

1. Introduction

Structural dynamics modification technology is an economical and effective means for the improvement and enhancement of the dynamic characteristics of mechanical structures. It is widely used in aerospace, ships, automobiles, civil engineering, bridges, and machinery industries. The problems involved in structural dynamics modification can be divided into two categories: "forward problems" and "inverse problems". The former mainly involves changes in the dynamic characteristics of the structure due to changes to the mass, stiffness, and damping of the original structure; the latter mainly comprises the study of how to modify the existing structure in order to achieve the expected dynamic characteristics (natural frequencies and mode shapes) [1–5]. Compared to "forward problems", "inverse problems" are attracting more and more research due to their complexity and extensive engineering application value [6].

One of the important sub-problems in the "inverse problem" of structural dynamics modification is known as the assignment of natural frequencies and modes, which refers to the modification of the structure to make the system meet certain frequency characteristics or modal requirements. For example, in many engineering applications, it is desirable for some of the system's natural frequencies to be far away from the dominant components of the harmonic excitation force, in order to prevent resonance that may lead to structural failure. Bycontrast, in other cases, such as the design of resonators, it is desirable for the natural frequency of the system to match the single-harmonic excitation, in order to improve the performance of the machine and, at the same time, minimize the excitation effort [7]. For military aircraft, such as airplanes, rockets, and missiles, not only the natural frequency requirements of the structure need to be considered in the design, but also certain requirements for the position of the modal nodes of the structure. For example, in the structural design of a vehicle, if the installation position of the attitude sensor can be located at the first few modes of the structure through the optimization design, the vibration level of the attitude sensor can be effectively reduced and the attitude detection accuracy can be improved. In the early research on the assignment of natural frequencies and mode shapes, most are summarized as system-characteristic structural assignment problems. Syrmos et al. [8,9] studied these problems and presented numerical solutions. Gobb and Liebst [10] considered the application of the eigenstructural assignments of the undamped structural system in mechanics. This method is similar to that of adding stiffness to the original structure in recent structural modifications. Fletcher et al. [11–15] studied the assignment problems of the state feedback eigenstructure of the descriptor system. They also discussed the assignment problems posed by the eigenvalue structure of the output feedback of the descriptor system in the work of Duan and Fletcher, respectively [16,17]. Duan and Patton [18] studied the robustness eigenstructure assignment problems of the descriptor system. Again, the concept in these studies of descriptor systems is similar to the idea of adding masses and stiffness to the original structure in recent structural modifications. In 2004, Kyprianou, et al. [19] proposed a natural frequency assignment method. The main features of this method are the addition of mass and one or more stiffness to the original structure, and that the determination of the added mass or stiffness required by the receptance of the original structural system. Mottershead et al. [20] used the receptance measured by the vibration system to assign the eigenvalues of the vibration's differential equation through active vibration control and passive structure modification. In order to draw a comparison with the results of the well-established technique proposed by Braun and Ram, Ouyang et al. [21] developed a method that relied only on receptance data for the calculation of the realizable mass and stiffness modification of undamped systems. In 2013, Mao and Dai [22] proposed a partial eigenvalue assignment method for linear high-order systems. They established a new orthogonal relationship between the eigenvectors of general matrix polynomials. By using this new orthogonal relationship, the parameter solution of partial eigenvalue assignment was constructed, and the eigenvalues that needed to be modified were assigned, while the eigenvalues that did not need to be modified remained unchanged. The characteristic feature of this method was that the eigenvalues that did not need to be modified were ignored. Hu et al. [23] proposed an approach to the partial eigenvalue and eigenstructure assignment of undamped vibrating systems. This approach only needed a few eigenpairs to be assigned, as well as the mass and stiffness matrices of the open-loop vibration system. In 2015, Ouyang et al. [24] studied a method for the assignment of some natural frequencies on the mass-spring system; the most important aspect of this method was that, when natural frequencies were assigned, other natural frequencies that did not need to be assigned did not change. This phenomenon was called "no spill-over". In the same year, an eigenstructure assignment method based on receptance was proposed by Liu et al. [25]. The core component of this method was the addition of spring-mass subsystems to the original structure, followed by the transformation of the eigenstructure assignment problems into numerical optimization problems. One year later, Belotti et al. [26] proposed an inverse structure modification method for eigenstructure assignment. The proposed method allowed the assignment of the desired modes only at the parts of interest of the system, according to an arbitrary number of modification parameters and determined eigenpairs. In 2017, Bai et al. [27] analyzed the assignment problem of local quadratic eigenvalues in vibration through active feedback control. A constructive method was proposed to solve the local quadratic eigenvalue assignment problem based on the measured receptance and the system parameter matrix. The solution to the problem required only a small linear system and a few unwanted eigenvalues with related eigenvectors. One year later, in order to assign a certain number of natural frequencies, a numerical method based on the Sherman-Morrison formula was proposed [28]. This method required the receptance values related to the modified coordinates of the original system structure. In 2018, Belotti et al. [29] proposed a method that aimed to assign a subset of natural frequencies with low spill-over. In 2020, Tsai et al. [30] proposed a theoretical study of frequency assignment for the coupling system. This method was capable of solving some complex modification issues, in which the added structures were not point mass or ground springs.

The above-mentioned studies on the assignment of frequencies and modes were primarily based on the physical model, which requires the knowledge of mass, stiffness, and damping matrices. In practical engineering, however, these parameters and matrices of vibration system structures are not easy to obtain. Although there are a few FRF-based assignment methods, they can only be applied with specific modifications, such as only adding mass, or only adding spring stiffness. In addition, most of the above studies only considered the frequency assignment, ignoring the assignment of the mode shapes. This paper proposes a method for structural modifications for the assignment of natural frequencies and mode shapes based on FRFs. Multiple modification schemes were considered in this study, including the addition of masses or stiffness (supporting stiffness or connection stiffness between different coordinates), the addition of masses and stiffness simultaneously, or the addition of mass-spring substructures to the original structure. Firstly, the proposed technique was formulated as an optimization problem based on the FRFs of the original structure and the masses or stiffness that needed to be added. Next, the required added masses and stiffness were obtained by solving the optimization model using a genetic algorithm. The advantage of this FRFs-based method is that the FRFs can be directly measured by modal testing, without knowledge of analytical or modal models. Furthermore, multiple structural modification schemes were considered for the assignment of the natural frequencies and mode shapes, making this method more applicable to engineering and more likely to achieve better results.

2. Theoretical Development

Although damping always exists, it is relatively small in most engineering structures. Even if a damping ratio is 10%, the difference between a damped natural frequency and an undamped natural frequency is only 0.5% [25]. Therefore, damping is ignored in the following theoretical analysis. As shown in Figure 1, an undamped n-degree-of-freedom (DOF) system was considered. The dynamics of the vibrating structure were modeled by the following the second-order differential equation:

$$\mathbf{M}\ddot{\mathbf{x}} + \mathbf{K}\mathbf{x} = 0 \tag{1}$$

where $\ddot{\mathbf{x}}$ and $\mathbf{x}$ are the acceleration and displacement vector, respectively. $\mathbf{M}$, $\mathbf{K}\in\mathbf{R}^{n\times n}$ are the mass and stiffness matrices respectively. It is well known that if $\mathbf{x} = \mathbf{u}e^{i\omega t}$ is a fundamental solution to Equation (1), then the vibration's differential Equation (1) is transformed from a time domain to a frequency domain. Equation (1) was therefore rewritten as follows:

$$\left(-\mathbf{M}\omega^2 + \mathbf{K}\right)\mathbf{u} = 0 \tag{2}$$

where ω is the natural frequency of the spring-mass vibration system and $\mathbf{u}$ is the mode shapes. Dynamic modification was introduced to the original structure through the addition of masses or stiffness to the positions of the system, and the added mass and stiffness matrices were $\Delta\mathbf{M}$ and $\Delta\mathbf{K}$, respectively. The vibration's differential equation in the time domain of the modified structural system was described as follows:

$$\left[-\omega^2(\mathbf{M} + \Delta\mathbf{M}) + (\mathbf{K} + \Delta\mathbf{K})\right]\mathbf{u} = 0 \tag{3}$$

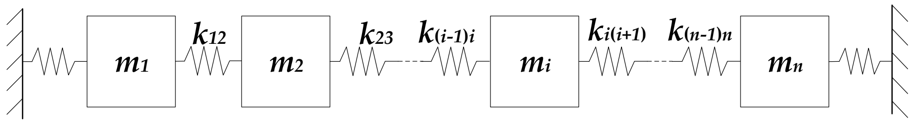

Figure 1. n-degree-of-freedom undamped vibration system.

As for the original structural system, the dynamic stiffness matrix and the receptance matrix in the frequency domain were represented by $\mathbf{Z}(\omega)$ and $\mathbf{H}(\omega)$, respectively. They were represented by the mass and stiffness matrix as follows:

$$\mathbf{Z}(\omega) = \left(-\omega^2\mathbf{M} + \mathbf{K}\right)$$
$$\mathbf{H}(\omega) = \left(-\omega^2\mathbf{M} + \mathbf{K}\right)^{-1}$$

Therefore, Equation (3) was described by the receptance matrix of the original structural system. The result is shown in Equation (4):

$$\mathbf{H}^{-1}(\omega)\mathbf{u} = \left(\omega^2\Delta\mathbf{M} - \Delta\mathbf{K}\right)\mathbf{u} \tag{4}$$

Considering some of the limitations of structural modification in actual engineering, various structural modification schemes, including the addition of masses, stiffness, and mass-spring substructures are considered, respectively, in the following sections.

2.1. Addition of Masses

Assuming that a mass with a value dm_i is added onto the coordinate i of the original structural system, as shown in Figure 2, the consequent vibration's differential equation can be described by Equation (5).

$$\mathbf{H}_{n\times n}^{-1}\begin{pmatrix} u_1 \\ u_2 \\ \vdots \\ u_i \\ \vdots \\ u_n \end{pmatrix} = \omega^2 \cdot \Delta\mathbf{M}_i \begin{pmatrix} u_1 \\ u_2 \\ \vdots \\ u_i \\ \vdots \\ u_n \end{pmatrix} = \begin{pmatrix} 0 & 0 & \cdots & 0 & \cdots & 0 \\ 0 & 0 & \cdots & 0 & \cdots & 0 \\ \vdots & \vdots & \ddots & \vdots & & \vdots \\ 0 & 0 & \cdots & \omega^2 dm_i & \cdots & 0 \\ \vdots & \vdots & & \vdots & \ddots & \vdots \\ 0 & 0 & \cdots & 0 & \cdots & 0 \end{pmatrix}\begin{pmatrix} u_1 \\ u_2 \\ \vdots \\ u_i \\ \vdots \\ u_n \end{pmatrix} \tag{5}$$

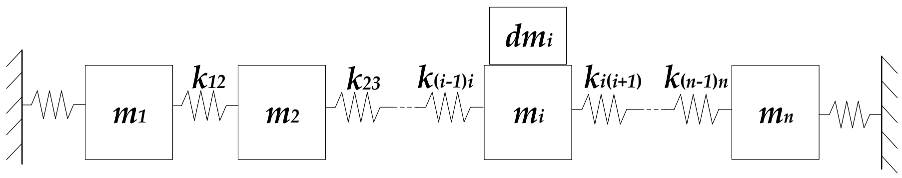

Figure 2. Structural modification by adding mass.

In some specific structures, it is impossible for the designer to add masses in order to improve the dynamic characteristics of the structure. For example, some barrel-shaped or beam structures [31] are not allowed to change their appearance due to functional requirements. Under these conditions, the addition of stiffness can be considered. In Sections 2.2 and 2.3, two forms are discussed, including the addition of supporting stiffness and the addition of connection stiffness, respectively.

2.2. Addition of Supporting Stiffness

Assuming that a supporting stiffness with a value dk_i is added onto the coordinate i of original system, as shown in Figure 3, the vibration's differential equation after adding stiffness dk_i can be described by Equation (6). It is not surprising that Equation (5) is similar to the Equation (5) presented by Kyprianou, et al. [19] when $\delta\mathbf{K} = 0$, and Equation (6) is similar to the Equation (5) presented by Kyprianou, et al. [19] when $\delta\mathbf{M} = 0$.

$$\mathbf{H}_{n\times n}^{-1}\begin{pmatrix} u_1 \\ u_2 \\ \vdots \\ u_i \\ \vdots \\ u_n \end{pmatrix} = -\Delta\mathbf{K}_i\begin{pmatrix} u_1 \\ u_2 \\ \vdots \\ u_i \\ \vdots \\ u_n \end{pmatrix} = \begin{pmatrix} 0 & 0 & \cdots & 0 & \cdots & 0 \\ 0 & 0 & \cdots & 0 & \cdots & 0 \\ \vdots & \vdots & \ddots & \vdots & & \vdots \\ 0 & 0 & \cdots & -dk_i & \cdots & 0 \\ \vdots & \vdots & & \vdots & \ddots & \vdots \\ 0 & 0 & \cdots & 0 & \cdots & 0 \end{pmatrix}\begin{pmatrix} u_1 \\ u_2 \\ \vdots \\ u_i \\ \vdots \\ u_n \end{pmatrix} \tag{6}$$

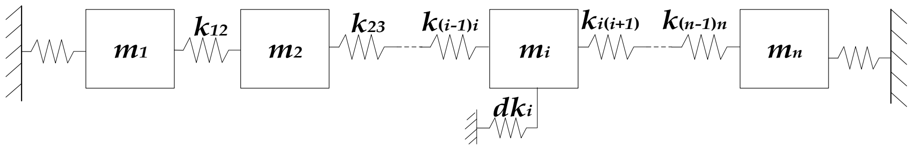

Figure 3. Structural modification by adding supporting stiffness.

2.3. Addition of Connection Stiffness

Assuming a connection stiffness with value dk_{ij} is added between the coordinate i and coordinate j of original system, as shown in Figure 4, the vibration's differential equation after the addition of connection stiffness dk_{ij} can be described by Equation (7):

$$\mathbf{H}_{n\times n}^{-1}\begin{pmatrix} u_1 \\ u_2 \\ \vdots \\ u_i \\ \vdots \\ u_j \\ \vdots \\ u_n \end{pmatrix} = -\Delta\mathbf{K}_{ij}\begin{pmatrix} u_1 \\ u_2 \\ \vdots \\ u_i \\ \vdots \\ u_j \\ \vdots \\ u_n \end{pmatrix} = \begin{pmatrix} 0 & 0 & \cdots & 0 & \cdots & 0 & \cdots & 0 \\ 0 & 0 & \cdots & 0 & \cdots & 0 & \cdots & 0 \\ \vdots & \vdots & \ddots & \vdots & & \vdots & & \vdots \\ 0 & 0 & \cdots & -dk_{ij} & \cdots & dk_{ij} & \cdots & 0 \\ \vdots & \vdots & & \vdots & \ddots & \vdots & \vdots & \vdots \\ 0 & 0 & \cdots & dk_{ij} & \cdots & -dk_{ij} & \cdots & 0 \\ \vdots & \vdots & & \vdots & & \vdots & \ddots & \vdots \\ 0 & 0 & \cdots & 0 & \cdots & 0 & \cdots & 0 \end{pmatrix}\begin{pmatrix} u_1 \\ u_2 \\ \vdots \\ u_i \\ \vdots \\ u_j \\ \vdots \\ u_n \end{pmatrix} \tag{7}$$

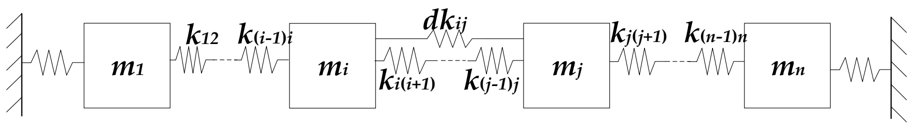

Figure 4. Structural modification by adding connection stiffness between different coordinates.

2.4. Addition of Spring-Mass Substructure

In some cases, the original structure was designed for certain specific functions and requirements, which were not to be modified. In these cases, adding spring-mass substructures to the original system was a preferable structural modification scheme for the improvement of the system's dynamic characteristics.

It was assumed that a spring-mass substructure with mass dm_i and stiffness dk_i was added onto coordinate i of the original structural system, as shown in Figure 5. Due to the addition of this spring-mass substructure, an extra DOF was introduced. Consequently, the matrices in Equation (4) were enlarged by one row and column, as shown in Equation (8).

$$\begin{pmatrix} \mathbf{H}_{n\times n}^{-1} & 0 \\ 0 & 0 \end{pmatrix}\begin{pmatrix} u_1 \\ u_2 \\ \vdots \\ u_i \\ \vdots \\ u_n \\ du \end{pmatrix} = \begin{pmatrix} 0 & 0 & \cdots & 0 & \cdots & 0 & 0 \\ 0 & 0 & \cdots & 0 & \cdots & 0 & 0 \\ \vdots & \vdots & \ddots & \vdots & & \vdots & \vdots \\ 0 & 0 & \cdots & -dk_i & \cdots & 0 & dk_i \\ \vdots & \vdots & & \vdots & \ddots & \vdots & \vdots \\ 0 & 0 & \cdots & 0 & \cdots & 0 & 0 \\ 0 & 0 & \cdots & dk_i & \cdots & 0 & -dk_i + \omega^2 dm_i \end{pmatrix}\begin{pmatrix} u_1 \\ u_2 \\ \vdots \\ u_i \\ \vdots \\ u_n \\ du \end{pmatrix} \tag{8}$$

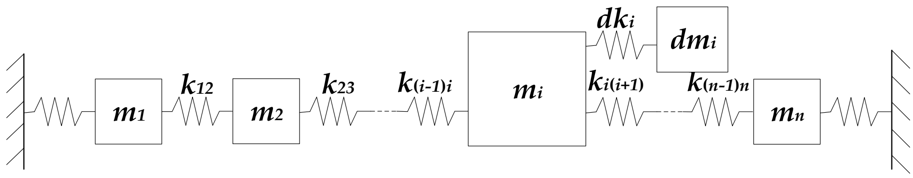

Figure 5. Structural modification by adding spring-mass substructure.

According to the last row of Equation (8), one can obtain

$$\left(\omega^2 dm_i - dk_i\right) du + dk_i u_i = 0 \tag{9}$$

Solving for du in terms of u_i yields

$$du = \left(\frac{dk_i}{dk_i - \omega^2 dm_i}\right) u_i \tag{10}$$

Substituting Equation (10) into Equation (8), the right side of Equation (8) can be written as follows:

$$\begin{pmatrix} 0 & 0 & \cdots & 0 & \cdots & 0 & 0 \\ 0 & 0 & \cdots & 0 & \cdots & 0 & 0 \\ \vdots & \vdots & \ddots & \vdots & & \vdots & \vdots \\ 0 & 0 & \cdots & -dk_i & \cdots & 0 & dk_i \\ \vdots & \vdots & & \vdots & \ddots & \vdots & \vdots \\ 0 & 0 & \cdots & 0 & \cdots & 0 & 0 \\ 0 & 0 & \cdots & dk_i & \cdots & 0 & -dk_i + \omega^2 dm_i \end{pmatrix}\begin{pmatrix} u_1 \\ u_2 \\ \vdots \\ u_i \\ \vdots \\ u_n \\ \left(\frac{dk_i}{dk_i - \omega^2 dm_i}\right) u_i \end{pmatrix} \tag{11}$$

Considering the ith and (n + 1)th row of Equation (11), one can obtain

$$\begin{gathered} -dk_i\ u_i + \left(\frac{(dk_i)^2}{dk_i - \omega^2 dm\ _i}\right) u_i = \left(\frac{\omega^2 dm_i dk_i}{dk_i - \omega^2 dm_i}\right) u_i \\ dk_i\ u_i + \left(\frac{\omega^2 dm_i - dk_i}{dk_i - \omega^2 dm_i}\right) dk\ _i u_i = 0 \end{gathered} \tag{12}$$

Combining Equations (10)–(13), Equation (9) can be simplified as equation

$$\mathbf{H}_{n\times n}^{-1}\begin{pmatrix} u_1\\ u_2\\ \vdots\\ u_i\\ \vdots\\ u_n \end{pmatrix} = -\Delta\mathbf{S}_i\begin{pmatrix} u_1\\ u_2\\ \vdots\\ u_i\\ \vdots\\ u_n \end{pmatrix} = \begin{pmatrix} 0 & 0 & \cdots & 0 & \cdots & 0\\ 0 & 0 & \cdots & 0 & \cdots & 0\\ \vdots & \vdots & \ddots & \vdots & & \vdots\\ 0 & 0 & \cdots & \frac{\omega^2 dm_i dk_i}{dk_i-\omega^2 dm_i} & \cdots & 0\\ \vdots & \vdots & & \vdots & \ddots & \vdots\\ 0 & 0 & \cdots & 0 & \cdots & 0 \end{pmatrix}\begin{pmatrix} u_1\\ u_2\\ \vdots\\ u_i\\ \vdots\\ u_n \end{pmatrix} \tag{13}$$

It is not surprising that Equation (13) is the same as Equation (11) in Liu, et al.'s study [25] when the force vector $\boldsymbol{f}$ = 0.

2.5. Expression of General Structural Modification

Combining the various structural modification schemes in Section 2.1, Section 2.2, Section 2.3 and Section 2.4, we were able to obtain the general structural modification expression. It was assumed that extra mass dm_i was added onto the ith coordinate, the supporting stiffness dk_j was added onto the coordinate j, connecting stiffness dk_{pq} was added between the pth and the qth coordinates, and a spring-mass substructure with a mass value dm_m and a stiffness value dk_m was added onto the coordinate m of the original system, as shown in Figure 6. According to Equations (5)–(7), the general expression of the vibration's differential equation for the modified structure was derived, as shown in Equation (14).

$$\mathbf{H}_{n\times n}^{-1}\begin{pmatrix} u_1\\ \vdots\\ u_i\\ u_j\\ u_{pq}\\ \vdots\\ u_{pq}\\ u_m\\ \vdots\\ u_n \end{pmatrix} = \begin{pmatrix} 0 & \cdots & 0 & 0 & 0 & \cdots & 0 & 0 & \cdots & 0\\ \vdots & \ddots & & & & & & & & \vdots\\ 0 & \cdots & \omega^2 dm_i & & & & & & \cdots & 0\\ 0 & \cdots & & -dk_j & & & & & \cdots & 0\\ 0 & \cdots & & & -dk_{pq} & & dk_{pq} & & \cdots & 0\\ \vdots & \vdots & & & \vdots & \ddots & \vdots & & \vdots & \vdots\\ 0 & \cdots & & & dk_{pq} & & -dk_{pq} & & \cdots & 0\\ 0 & \cdots & 0 & 0 & 0 & 0 & 0 & \frac{\omega^2 dm_m dk_m}{dk_m-\omega^2 dm_m} & \cdots & 0\\ \vdots & \vdots & \vdots & \vdots & \vdots & \vdots & \vdots & \vdots & \ddots & \vdots\\ 0 & \cdots & 0 & 0 & 0 & \cdots & 0 & 0 & \cdots & 0 \end{pmatrix}\begin{pmatrix} u_1\\ \vdots\\ u_i\\ u_j\\ u_{pq}\\ \vdots\\ u_{pq}\\ u_m\\ \vdots\\ u_n \end{pmatrix} \tag{14}$$

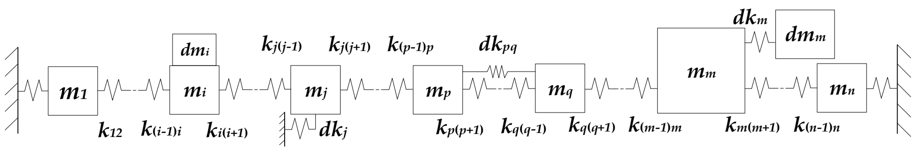

Figure 6. General structural modification.

2.6. Establishment of Optimization Model

In order to establish a unified optimization model, the added mass matrix $\Delta\mathbf{M}_i$ in Equation (5), the added supporting stiffness matrix $\Delta\mathbf{K}_i$ in Equation (6), the added connection stiffness matrix $\Delta\mathbf{K}_{ij}$ in Equation (7), and the added substructure matrix $\Delta\mathbf{S}_i$ in Equation (13) were converted into the form of Equations (15)–(18), respectively:

$$\begin{gathered} \Delta\mathbf{M}_i = dm_i \mathbf{V}_m^i {\mathbf{V}_m^i}^T\\ \mathbf{V}_m^i = \begin{pmatrix} 0 & \cdots & 0 & \underset{i}{1} & 0 & \cdots & 0 \end{pmatrix}^T \end{gathered} \tag{15}$$

$$
\begin{gathered}
\Delta \mathbf{K}_i = dk_i \mathbf{V}_k^i \mathbf{V}_k^{i\,T} \\
\mathbf{V}_k^i = \begin{pmatrix} 0 & \cdots & 0 & \underset{i}{1} & 0 & \cdots & 0 \end{pmatrix}^T
\end{gathered} \tag{16}
$$

$$
\begin{gathered}
\Delta \mathbf{K}_{ij} = dk_{ij} \mathbf{V}_k^{ij} \mathbf{V}_k^{ij\,T} \\
\mathbf{V}_k^{ij} = \begin{pmatrix} 0 & \cdots & 0 & \underset{i}{1} & 0 & \cdots & 0 & \underset{j}{-1} & 0 & \cdots & 0 \end{pmatrix}^T
\end{gathered} \tag{17}
$$

where the added stiffness dk_{ij} represents the connection stiffness between the coordinates i and coordinate j when $i \neq j$. If $i = j$, dk_{ij} represents the supporting stiffness corresponding with the coordinate i, and

$$
\begin{gathered}
\mathbf{V}_k^{ij} = \left(0 \cdots 0 \underset{i}{1} 0 \cdots 0\right)^T \\
\Delta \mathbf{S}_i = ds_i \mathbf{V}_s^i \mathbf{V}_s^{i\,T} \\
ds_i = -\frac{\omega^2 dm_i dk_i}{dk_i - \omega^2 dm_i} \\
\mathbf{V}_s^i = \left(0 \cdots 0 \underset{i}{1} 0 \cdots 0\right)^T
\end{gathered} \tag{18}
$$

For the sake of generalization, it was assumed that masses were added onto the first s coordinates, stiffness were added onto the first t coordinates, and the spring-mass substructures were added onto the first l coordinates of the original structure. By combining Equations (15)–(18), the vibration's differential equation in the modified structural system was described as Equation (19):

$$
\begin{gathered}
\left(\left(\mathbf{K} - \omega^2 \mathbf{M} \right) - \omega^2 \sum_{i=1}^{s} dm_i \mathbf{V}_m^i \mathbf{V}_m^{i\,T} + \sum_{i=1}^{t} dk_{ij} \mathbf{V}_k^{ij} \mathbf{V}_k^{ij\,T} + \sum_{i=1}^{l} ds_i \mathbf{V}_s^i \mathbf{V}_s^{i\,T} \right) \mathbf{u} = 0 \\
j \in [1, t]
\end{gathered} \tag{19}
$$

Set:

$$
\begin{gathered}
\boldsymbol{\alpha} = \left(-\omega^2 dm_1, -\omega^2 dm_2 \ldots - \omega^2 dm_s; dk_{1j}, dk_{2j} \ldots dk_{tj}; ds_1, ds_2 \ldots ds_l \right)^T \\
\mathbf{V} = \left(\mathbf{V}_m^{1\,T}, \mathbf{V}_m^{2\,T} \ldots \mathbf{V}_m^{s\,T}, \mathbf{V}_k^{1j\,T} \ldots \mathbf{V}_k^{tj\,T}, \mathbf{V}_s^{1\,T} \ldots \mathbf{V}_s^{l\,T} \right)^T \\
j \in [1, t]
\end{gathered} \tag{20}
$$

Equation (20) was simply described as follows:

$$
\left(\left(\mathbf{K} - \omega^2 \mathbf{M} \right) + \sum_{i=1}^{r} \alpha_i \mathbf{V}_i \mathbf{V}_i^{\,T} \right) \mathbf{u} = 0 \tag{21}
$$

where $r = s + t + l$, α_i is the element in the ith row of vector $\boldsymbol{\alpha}$ and $\mathbf{V}_i$ represents the ith column of the matrix $\mathbf{V}$.

As in Equation (4), Equation (21) was described by using the receptance matrix of the original system, as shown in Equation (22):

$$
\mathbf{H}^{-1}(\omega) \mathbf{u} = -\sum_{i=1}^{r} \alpha_i \mathbf{V}_i \mathbf{V}_i^{\,T} \mathbf{u} \tag{22}
$$

By substituting the desired natural frequency ω_h and mode $\mathbf{u}_h$ into Equation (22), we obtained:

$$
\mathbf{u}_h = \mathbf{H}(\omega_h) \left(-\sum_{i=1}^{r} \alpha_i \mathbf{V}_i \mathbf{V}_i^{\,T} \right) \mathbf{u}_h \tag{23}
$$

Therefore, the assignment of natural frequencies and mode shapes in this paper was cast as an optimization problem, as shown in Equation (24):

$$\min_{\alpha_i}\left\{\sum_{h=1}^{n}\gamma_h\left\|\mathbf{H}(\omega_h)\left(-\sum_{i=1}^{r}\alpha_i\mathbf{V}_i\mathbf{V}_i^T\right)\mathbf{u}_h-\mathbf{u}_h\right\|_2^2\right\} \tag{24}$$

where γ_h is the weighting coefficient. ω_h and $\boldsymbol{u}_h$ represent the desired frequency and mode. $\mathbf{H}$ represents FRF matrix, which consisted of FRFs of the original structure. $\mathbf{H}$ (ω_h) is the value of FRF matrix at frequency ω_h.

The above optimization model (24) can be solved by various optimization algorithms and a genetic algorithm was employed in the following numerical verification. It should be noted that the algorithm for solving this optimization problem will not be discussed because it is not the focus of this paper. In order to describe the detailed process of assigning natural frequencies and modes, the schematic flow chart is presented as shown in Figure 7. The specific implementation process can be summarized by the following steps:

(1) We determined the frequencies and mode shapes that needed to be assigned, according to the actual engineering needs.
(2) We measured the FRFs of the original structure.
(3) We chose a suitable structural modification scheme (the addition of masses, supporting stiffness, connection stiffness, or substructures, or the addition of a mixture of these) and the corresponding ranges of the variables according to the actual conditions.
(4) We solved the optimal modification results according to the optimization model given in Equation (24) by using a genetic algorithm.

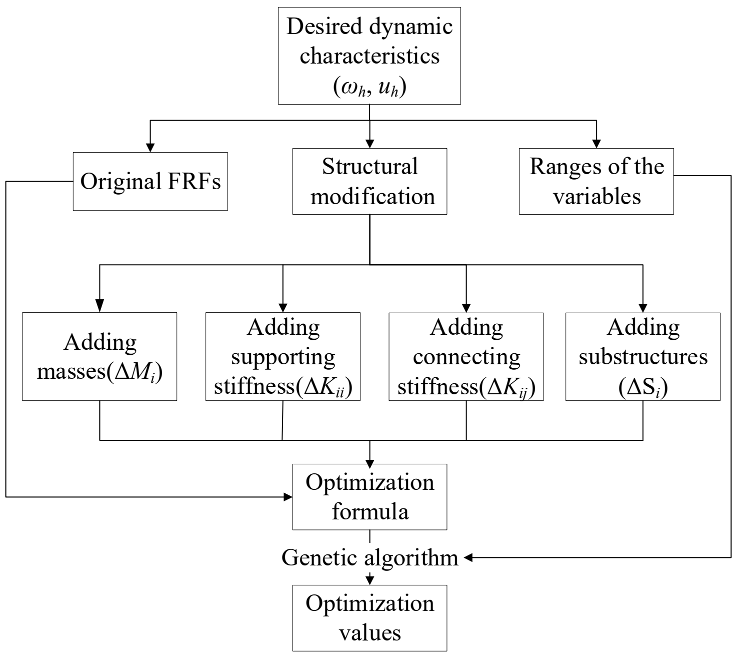

Figure 7. Complete schematic flow chart of assignment of natural frequencies and modes.

3. Verification of the Method

To verify the feasibility and accuracy of the proposed method, a 5-DOF undamped spring-mass system was presented as a simulated example, as shown in Figure 8. This simulated model was selected from a real example in a previous study [21]. Furthermore, all the system parameters, variation range of mass and stiffness, desired natural frequencies and mode shapes were also identical to those used in the same previous study [21]. The structural system parameters are listed in Table 1. Next, five natural frequencies and the corresponding mode shapes of this system were obtained, as summarized in Table 2. It should be noted that the natural frequencies and mode shapes of the system were directly numerically calculated in this simulated experiment, while in practical applications they should be extracted from the FRFs measured by experiment.

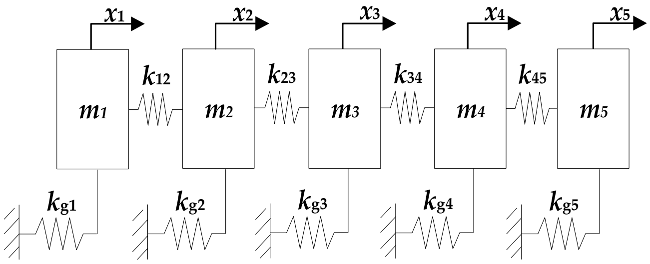

Figure 8. A 5-DOF undamped spring-mass vibration system.

Table 1. System parameters.

Stiffness (N/m)	k_{12} 7.36×10^4	k_{23} 6.82×10^4	k_{34} 7.35×10^4	k_{45} 8.21×10^4	k_g 9.89×10^4
Mass (kg)	m_1 1.73	m_2 5.12	m_3 8.21	m_4 2.61	m_5 1.34

Table 2. Natural frequencies of original structure.

Mode Number *i*	**1**	**2**	**3**	**4**	**5**
f_i (Hz)	22.28	32.61	42.94	52.74	64.59
u_i (1)	0.357	0.736	0.094	1.000	0.003
u_i (2)	0.673	1.000	0.060	−0.234	−0.004
u_i (3)	1.000	−0.418	−0.217	0.025	0.032
u_i (4)	0.460	−0.337	1.000	−0.008	−0.482
u_i (5)	0.244	−0.222	0.983	−0.019	1.000

The verification of the methods for the assignment of one natural frequency and mode shape and two natural frequencies and mode shapes is discussed in Sections 3.1 and 3.2, respectively. Desired natural frequencies and mode shapes are given in Table 3. The genetic algorithm toolbox in Matlab software was employed for solving this optimization problem. Default values were chosen as the input parameters of genetic algorithm. The inputs and the optimization termination criteria are given in Table 4.

Table 3. Desired natural frequencies and mode shapes.

Mode Number *d*	**1**	**2**
f_d (Hz)	39.00	55.00
u_d (1)	1.00	0
u_d (2)	−0.55	0.01
u_d (3)	0.2	−0.10
u_d (4)	0	0.80
u_d (5)	0.05	1.00

Table 4. Inputs and termination criteria.

Inputs of GA	
Population size	50 for 5 variables and 200 for 10 variables
Mutation function	Constraint dependent
Crossover function	Constraint dependent
Optimization Termination Criteria	
Generations	100 × number of variables
Stall generations	50
Function tolerance	1×10^{-6}
Constraint tolerance	1×10^{-3}

3.1. Assignment of One Natural Frequency and Mode

The assignment of one desired natural frequency and mode shape by different modification schemes is discussed in Sections 3.1.1–3.1.4.

3.1.1. Addition of Masses

As can be seen in Figure 9, it was assumed that masses dm_1, dm_2, dm_3, dm_4, and dm_5 were added to all the coordinates of the original system. The purpose of the modification was to assign the one mode listed in Table 3 at f_1 (39 Hz). The ranges of the added masses were both 0–2 kg. By solving the optimization Equation (24) using the genetic algorithm, the optimized values of the added masses and the minimized value were obtained, as collected in Table 5:

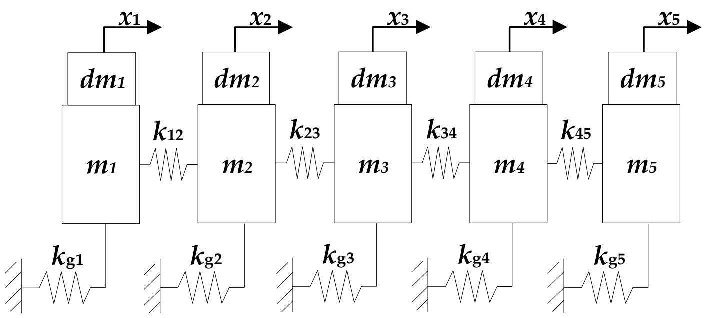

Figure 9. Modified structure after adding masses.

Table 5. Parameters of added masses.

Mass (kg)	Range	Value
dm_1	0–2	1.812
dm_2	0–2	1.189
dm_3	0–2	2.000
dm_4	0–2	0.358
dm_5	0–2	0
minimized value	0.03418162623201011	

As a further proof of the results, Figure 10 shows the absolute values of the receptance $H_{1,i}(\omega)$ (i = 1, . . . , 5) of the original system (solid line) and the modified systems by the proposed method (dotted line). For the purpose of comparison, the natural frequencies and the mode obtained from the modified system are collected in Table 6. In order to quantify the difference between the desired mode u_d and the attained mode u_i, the cosine 'cos'difference between them is given in the last row of Table 6. When the 'cos' value approached 1, the desired mode and the attained mode were very close. By contrast, the deviation was greater [25]. A graphical comparison of the desired and attained modes is also presented in order to make their difference more intuitive, as shown in Figure 11.

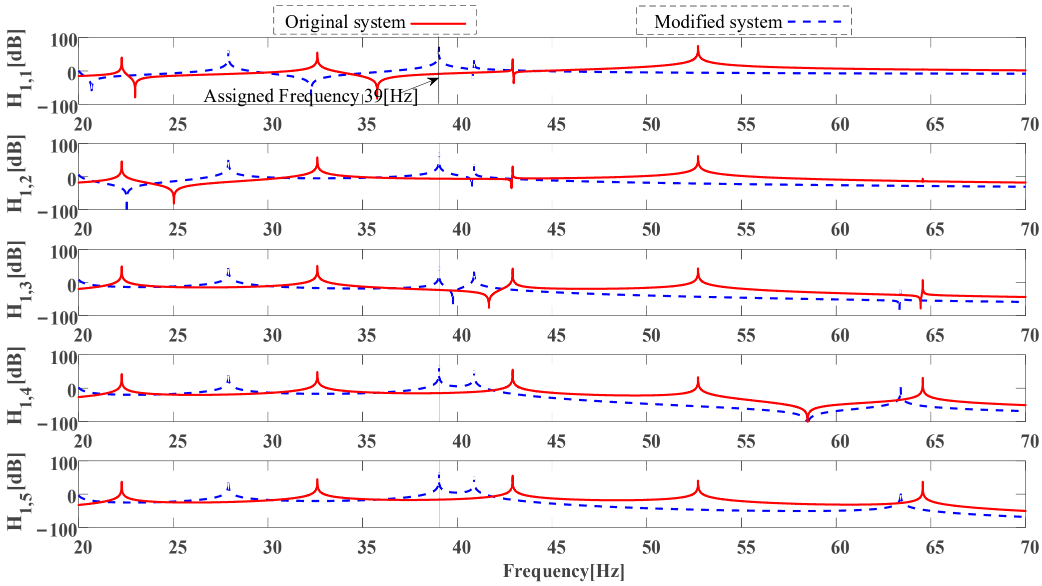

Figure 10. Original FRFs and FRFs after the addition of masses.

Table 6. Comparison of natural frequencies and mode shapes.

Frequency and Mode	Obtained	Frequency and Mode	Desired
f_i [Hz]	39.03	f_d [Hz]	39.00
u_i (1)	1	u_d (1)	1
u_i (2)	−0.5492	u_d (2)	−0.55
u_i (3)	0.0394	u_d (3)	0.2
u_i (4)	0.3092	u_d (4)	0
u_i (5)	0.2519	u_d (5)	0.05
Desired mode number, d		1	
$\lvert f_d - f_i \rvert (100 \times \lvert f_d - f_i \rvert / f_d)$		0.03 (0.08)	
cos (u_d,u_i)		0.9431	

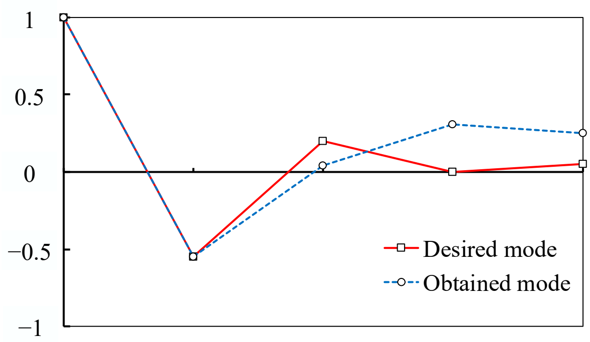

Figure 11. Comparison of desired and attained modes: 39 Hz.

3.1.2. Addition of Stiffness

The addition of supporting stiffness and connection stiffness is discussed in Sections 3.1.2.1 and 3.1.2.2.

3.1.2.1. Addition of Supporting Stiffness

As shown in Figure 12, it was assumed that supporting springs with stiffness dk_{11}, dk_{22}, dk_{33}, dk_{44}, dk_{55} were added to each coordinate of the original system. The purpose of the modification was to assign the one mode listed in Table 3 at f_2 (55 Hz). The ranges of the added stiffness were both 0~300 kN/m. By solving the optimization Equation (24) using the genetic algorithm, the optimized value of the added supporting stiffness and the minimized value were obtained, as listed in Table 7.

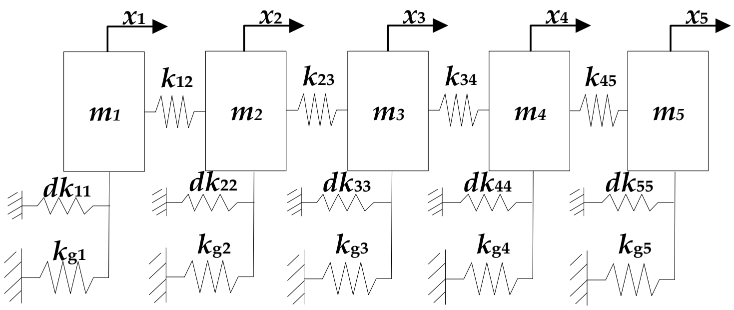

Figure 12. Modified structure after adding supporting stiffness.

Table 7. Parameters of added supporting stiffness.

Stiffness (kN/m)	Range	Value
dk_{11}	0–300	222.062
dk_{22}	0–300	4.798
dk_{33}	0–300	63.110
dk_{44}	0–300	156.854
dk_{55}	0–300	48.711
minimized value	0.008287571754663436	

The absolute values of the receptance $H_{1,i}(\omega)$ $(i = 1, \ldots, 5)$ of the original system (solid line) and the modified systems by the proposed method (dotted line) are shown in Figure 13. The natural frequencies and the mode obtained from the modified system are collected in Table 8. The difference between the cosine of the desired mode and the cosine of the attained mode is given in the last law of Table 8. A graphical comparison of the desired and attained modes is presented in Figure 14.

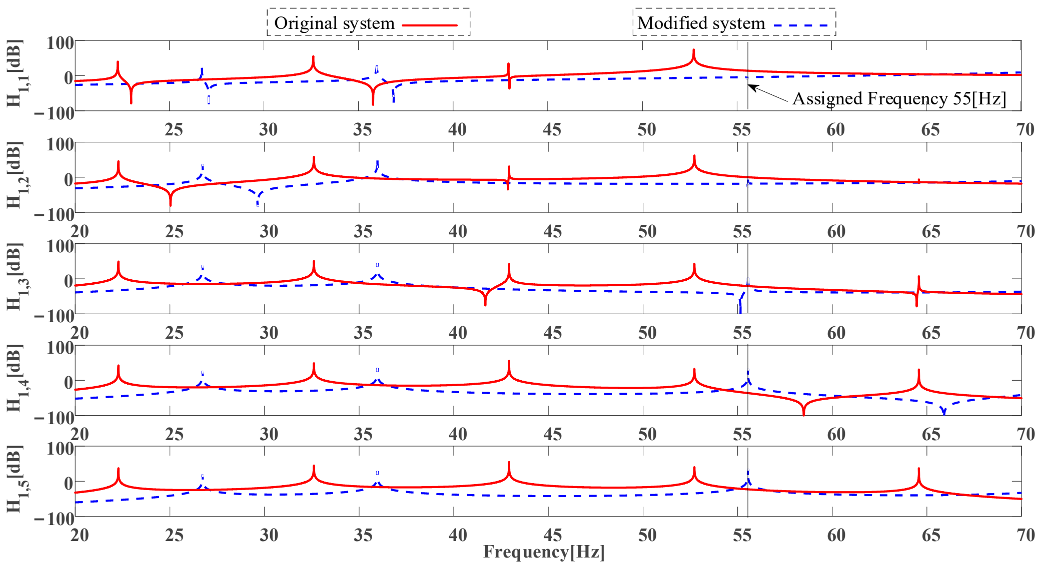

Figure 13. Original FRFs and FRFs after the addition of supporting stiffness.

Table 8. Comparison of natural frequencies and mode shapes.

Frequency and Mode	Obtained	Frequency and Mode	Desired
f_i [Hz]	55.55	f_d [Hz]	55.00
u_i (1)	0.0056	u_d (1)	0
u_i (2)	0.0147	u_d (2)	0.01
u_i (3)	−0.0869	u_d (3)	−0.10
u_i (4)	0.8102	u_d (4)	0.80
u_i (5)	1.00	u_d (5)	1.00
Desired mode number, d		2	
$\lvert f_d - f_i \rvert$ (100 × $\lvert f_d - f_i \rvert / f_d$)		0.55 (1.00)	
cos (u_d,u_i)		0.9999	

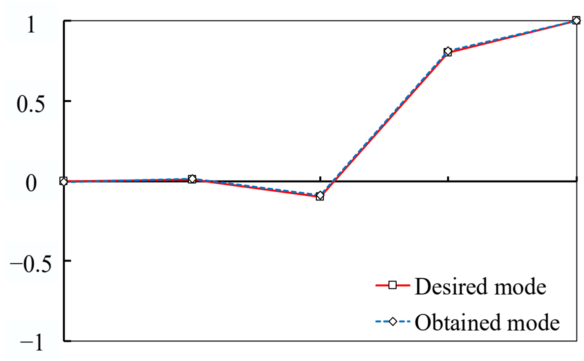

Figure 14. Comparison of desired and attained modes: 55 Hz.

3.1.2.2. Addition of Connection Stiffness

It is assumed that connection springs with stiffness dk_{13}, dk_{25}, dk_{14}, dk_{34} were added between the five coordinates of the original system, as shown in Figure 15. The purpose of the modification was to assign the one mode listed in Table 3 at f_2 (55 Hz). The ranges of the added stiffness were both 0~300 kN/m. By solving the optimization Equation (24) using the genetic algorithm, the optimized value of the added connection stiffness and the minimized value were obtained, as listed in Table 9.

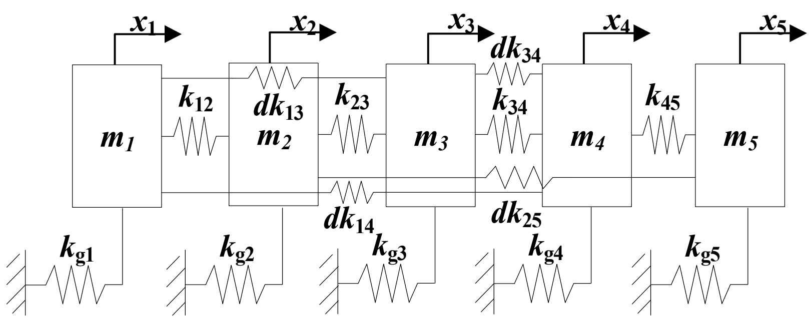

Figure 15. Modified structure after the addition of connection stiffness.

Table 9. Parameters of added connection stiffness.

Stiffness (kN/m)	Range	Value
dk_{13}	0–300	131.447
dk_{25}	0–300	44.234
dk_{14}	0–300	24.984
dk_{34}	0–300	87.119
minimized value	0.04288060323900754	

The absolute values of the receptance $H_{1,i}$ (ω) (i = 1, . . . , 5) of the original system (solid line) and the modified systems by the proposed method (dotted line) are shown in Figure 16. The natural frequencies and the mode obtained from the modified system are collected in Table 10. The difference between the cosine of the desired mode and the cosine of the attained mode is given in the last law of Table 10. A graphical comparison of the desired and attained modes is presented in Figure 17.

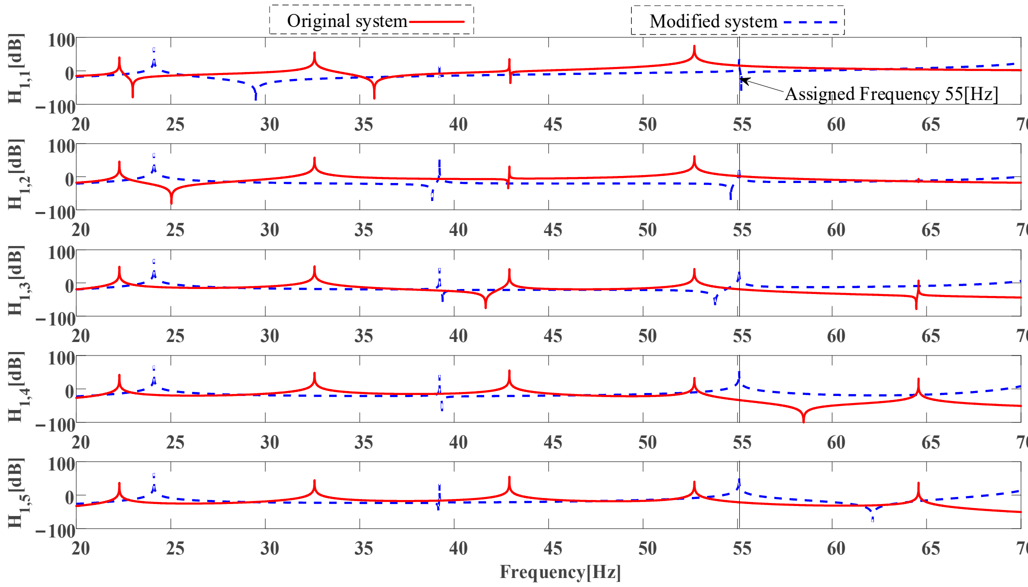

Figure 16. Original FRFs and FRFs after the addition of connection stiffness.

Table 10. Comparison of natural frequencies and mode shapes.

Frequency and Mode	Obtained	Frequency and Mode	Desired
f_i [Hz]	55.08	f_d [Hz]	55.00
u_i (1)	−0.1056	u_d (1)	0
u_i (2)	−0.0658	u_d (2)	0.01
u_i (3)	−0.2175	u_d (3)	−0.10
u_i (4)	0.8242	u_d (4)	0.80
u_i (5)	1.00	u_d (5)	1.00
Desired mode number, d		2	
$\lvert f_d - f_i \rvert$ ($100 \times \lvert f_d - f_i \rvert / f_d$)		0.08 (0.15)	
cos (u_d,u_i)		0.9911	

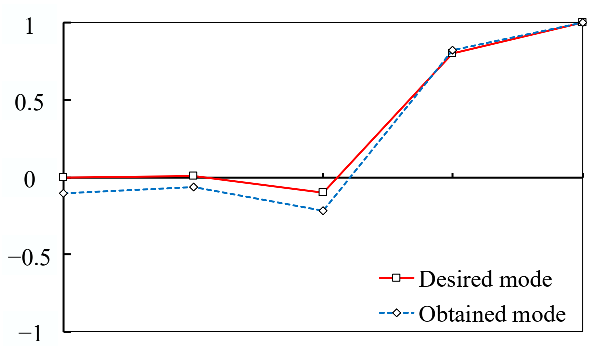

Figure 17. Comparison of desired and attained modes: 55 Hz.

3.1.3. Simultaneous Addition of Masses and Stiffness

It was assumed masses dm_1, dm_2, dm_3, dm_4, dm_5 and supporting stiffness dk_{11}, dk_{22}, dk_{33}, dk_{44}, dk_{55} were added to the original system simultaneously, as shown in Figure 18. The purpose of the modification was to assign the one mode listed in Table 3 at f_1 (39 Hz). The ranges of the added masses and stiffness were 0~2 kg and 0~300 kN/m, respectively. By solving the optimization Equation (24) using the genetic algorithm, the optimized value of the added supporting stiffness and masses and the minimized values were obtained, as listed in Table 11.

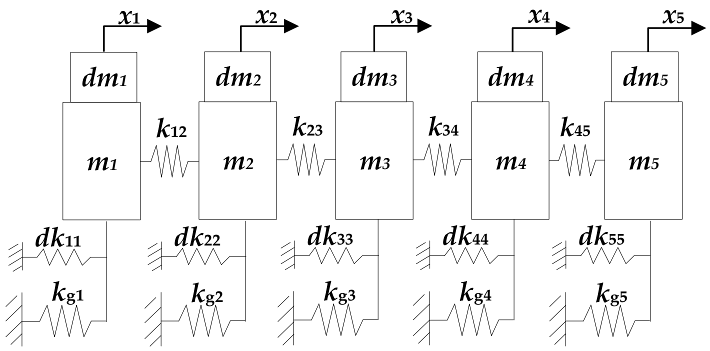

Figure 18. Modified structure after the simultaneous addition of masses and supporting stiffness.

Table 11. Parameters of added masses and supporting stiffness.

Mass (kg)	Range	Value	Stiffness (kN/m)	Range
dm_1	0–2	1.974	dk_{11}	0–300
dm_2	0–2	1.541	dk_{22}	0–300
dm_3	0–2	0.671	dk_{33}	0–300
dm_4	0–2	0.35	dk_{44}	0–300
dm_5	0–2	0.785	dk_{55}	0–300
minimized value		0.016437102458409666		

The absolute values of the receptance $H_{1,i}$ (ω) $(i = 1, \ldots, 5)$ of the original system (solid line) and the modified systems by the proposed method (dotted line) are shown in Figure 19. The natural frequencies and the mode obtained from the modified system are collected in Table 12. The difference between the cosine of the desired mode and cosine of the attained mode is given in the last law of Table 12. A graphical comparison of the desired and attained modes is presented in Figure 20.

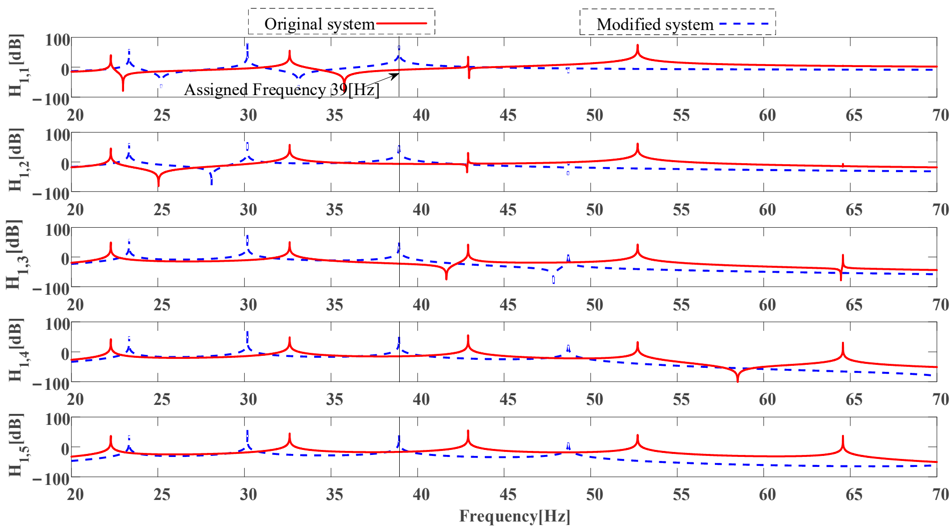

Figure 19. Original FRFs and FRFs after the simultaneous addition of masses and supporting stiffness.

Table 12. Comparison of natural frequencies and mode shapes.

Frequency and Mode	Obtained	Frequency and Mode	Desired
f_i [Hz]	38.94	f_d [Hz]	39.00
u_i (1)	1.00	u_d (1)	1.00
u_i (2)	−0.5493	u_d (2)	−0.55
u_i (3)	0.1341	u_d (3)	0.2
u_i (4)	0.0998	u_d (4)	0
u_i (5)	0.0275	u_d (5)	0.05
Desired mode number, d		1	
$\lvert f_d - f_i \rvert$ ($100 \times \lvert f_d - f_i \rvert / f_d$)		0.06 (0.15)	
cos (u_d,u_i)		0.9945	

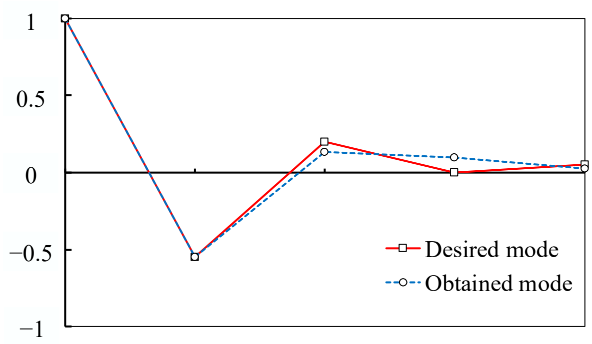

Figure 20. Comparison of desired and attained modes: 39 Hz.

3.1.4. Addition of Spring-Mass Substructures

It was assumed that spring-mass substructures with masses dm_1, dm_2, dm_3, dm_4, dm_5 and stiffness dk_{11}, dk_{22}, dk_{33}, dk_{44}, dk_{55} were added to original system, as shown in Figure 21. The purpose of the modification was to assign the one mode listed in Table 3 at f_1 (39 Hz). The ranges of the added masses and stiffness were 0~2 kg and 0~300 kN/m, respectively. By solving the optimization Equation (24) using the genetic algorithm, the optimized values of the substructures and the minimized value were solved and listed in Table 13.

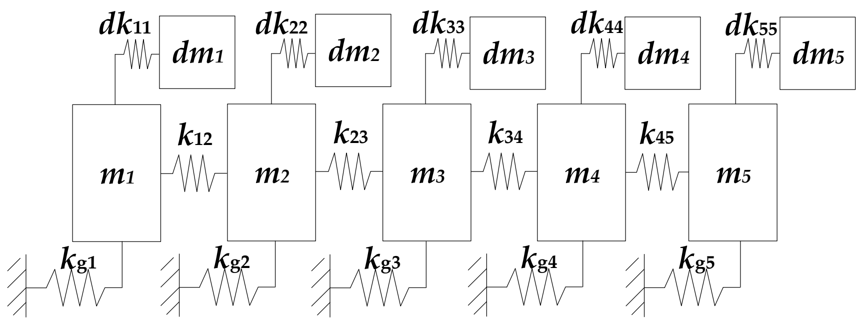

Figure 21. Modified structure after the addition of spring-mass substructures.

Table 13. Parameters of added masses and stiffness of the substructures.

Mass (kg)	Range	Value	Stiffness (kN/m)	Range	Value
dm_1	0–2	1.34	dk_{11}	0–300	280.005
dm_2	0–2	1.052	dk_{22}	0–300	279.597
dm_3	0–2	0.216	dk_{33}	0–300	279.268
dm_4	0–2	1.254	dk_{44}	0–300	163.297
dm_5	0–2	0.424	dk_{55}	0–300	21.965
minimized value			0.018034547178530872		

The absolute values of the receptance $H_{1,i}$ (ω) (i = 1, . . . , 5) of the original system (solid line) and the modified systems by the proposed method (dotted line) are shown in Figure 22. The natural frequencies and the mode obtained from the modified system are collected in Table 14. The difference between the cosine of the desired mode and the cosine of the attained mode is given in the last law of Table 14. A graphical comparison of the desired and attained modes is shown in Figure 23.

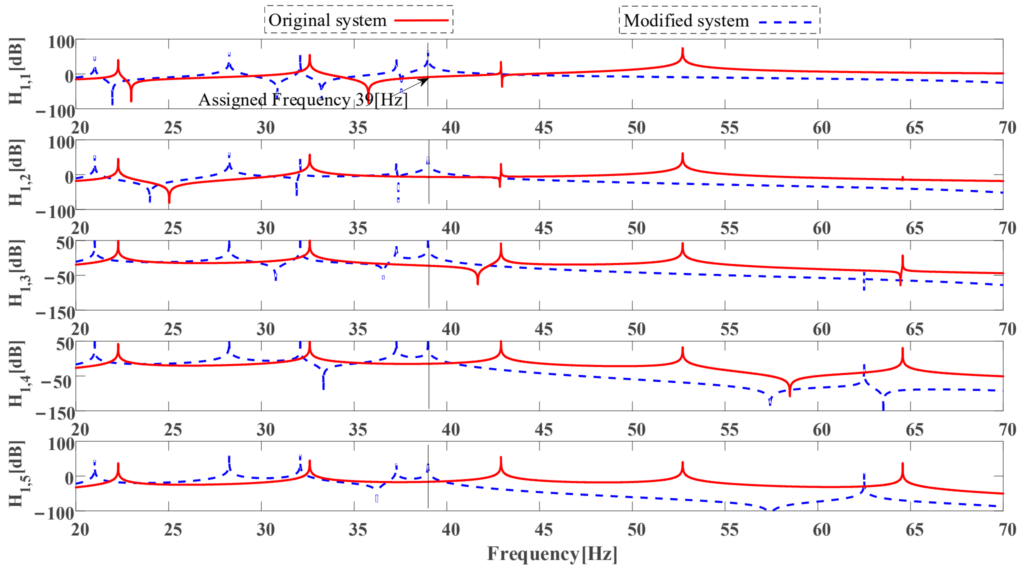

Figure 22. Original FRFs and FRFs after the addition of mass-spring substructures.

Table 14. Comparison of natural frequencies and mode shapes.

Frequency and Mode	Obtained	Frequency and Mode	Desired
f_i [Hz]	38.98	f_d [Hz]	39.00
u_i (1)	1.00	u_d (1)	1.00
u_i (2)	−0.5986	u_d (2)	−0.55
u_i (3)	0.2202	u_d (3)	0.2
u_i (4)	−0.2398	u_d (4)	0
u_i (5)	−0.0754	u_d (5)	0.05
Desired mode number, d		1	
$\lvert f_d - f_i \rvert (100 \times f_d - f_i \rvert / f_d)$		0.02 (0.05)	
cos (u_d,u_i)		0.9740	

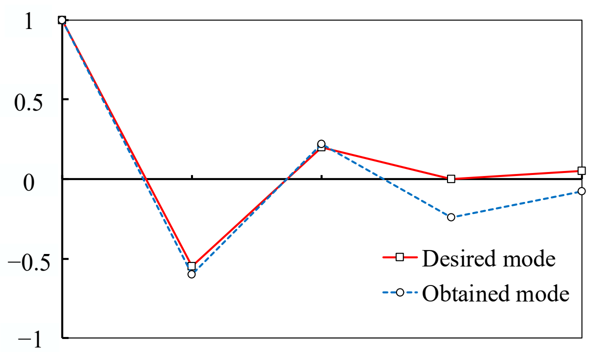

Figure 23. Comparison of desired and attained modes: 39 Hz.

3.2. Assignment of Two Natural Frequencies and Mode Shapes

In practical engineering, the assignment of only one natural frequency and mode usually cannot satisfy the characteristic requirements. Therefore, the assignment of two or multiple natural frequencies and mode shapes might be considered. In this section, the assignment of two natural frequencies and mode shapes (listed in Table 3) by different structural modifications schemes is discussed.

3.2.1. Addition of Masses

It was assumed that masses dm_1, dm_2, dm_3, dm_4, dm_5 were added to each coordinate of the original system, as shown in Figure 9. The goal of this modification was to assign the two vibration modes listed in Table 3. The ranges of the added masses were both 0~2 kg. By solving the optimization Equation (24) usng the genetic algorithm, the optimized values of the added masses and the minimized value were obtained, as listed in Table 15.

Table 15. Parameters of added masses.

Mass (kg)	Range	Value
dm_1	0–2	1.720
dm_2	0–2	1.425
dm_3	0–2	0
dm_4	0–2	0
dm_5	0–2	0
minimized value	1.71583241923l7873	

The absolute values of the receptance $H_{1,i}$ (ω) (i = 1, . . . , 5) of the original system (solid line) and the modified systems by the proposed method (dotted line) are shown in Figure 24. The natural frequencies and the mode obtained from the modified system are collected in Table 16. The difference between the cosine of the desired mode and the cosine of the attained mode is given in the last law of Table 16. A graphical comparison of the desired and attained modes is shown in Figure 25.

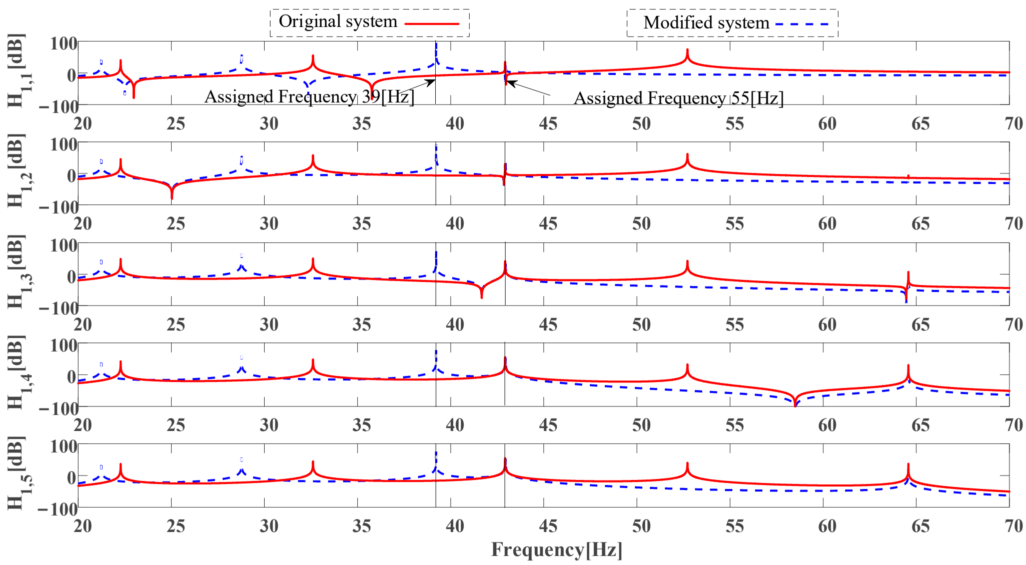

Figure 24. Original FRFs and FRFs after the addition of masses.

Table 16. Comparison of natural frequencies and mode shapes.

Frequency and Mode		Obtained	Frequency and Mode		Desired
f_i [Hz]	39.22	42.95	f_d [Hz]	39	39.22
u_i (1)	1.00	−0.086	u_d (1)	1.00	1.00
u_i (2)	−0.503	0.092	u_d (2)	−0.55	−0.503
u_i (3)	0.077	−0.227	u_d (3)	0.2	0.077
u_i (4)	0.198	1.016	u_d (4)	0	0.198
u_i (5)	0.163	1.000	u_d (5)	0.05	0.163
Desired mode number, d		1		2	
$\lvert f_d - f_i \rvert$ ($100 \times \lvert f_d - f_i \rvert / f_d$)		0.22 (0.56)		12.05 (21.91)	
cos (u_d,u_i)		0.9739		0.9866	

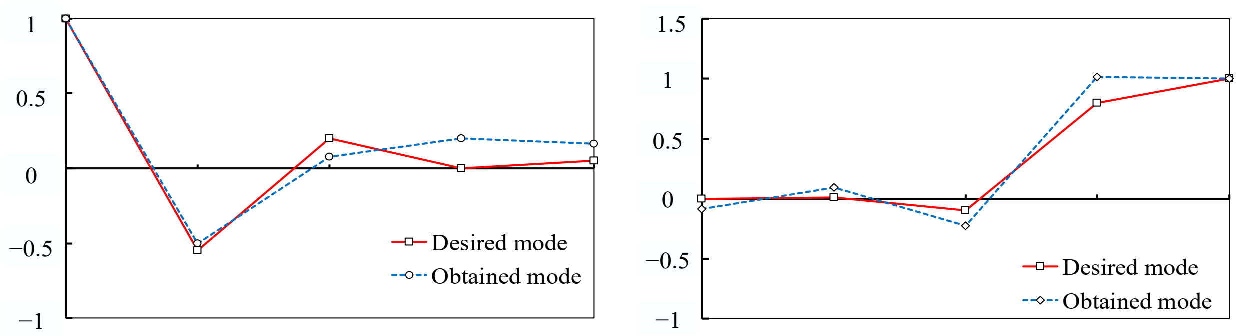

(**a**) (**b**)

Figure 25. Comparison of desired and attained modes: (**a**) 39 Hz; (**b**) 55 Hz.

The results shown in Table 16 demonstrate that the proposed method performed well in the assignment of frequency 39.00 Hz and the two desired modes, although the attained frequency of 42.95 Hz was far from the desired 55 Hz. We believe that this was because the number of desired modal parameters (two frequencies and ten mode elements) was much greater than that of modified variables (five added masses).

3.2.2. Addition of Supporting Stiffness

It was assumed that supporting springs with stiffness dk_{11}, dk_{22}, dk_{33}, dk_{44}, dk_{55} were added to each coordinate of the original system, as shown in Figure 12. The goal of this modification was to assign the two vibration modes listed in Table 3. The ranges of the added stiffness were both 0~300 kN/m. By solving the optimization Equation (24) using the genetic algorithm, the optimized value of the added supporting stiffness and the minimized value were obtained, as listed in Table 17.

Table 17. Parameters of supporting stiffness.

Stiffness (kN/m)	Range	Value
dk_{11}	0–300	0
dk_{22}	0–300	0
dk_{33}	0–300	54.065
dk_{44}	0–300	144.807
dk_{55}	0–300	52.889
minimized value	1.374314676701035469	

The absolute values of the receptance $H_{1,i}$ (ω) (i = 1, . . . , 5) of the original system (solid line) and the modified systems by the proposed method (dotted line) are shown in Figure 26. The natural frequencies and mode shapes obtained from the modified system are collected in Table 18. The difference between the cosine of the desired mode shapes and the cosine of the attained mode shapes is given in the last law of Table 18. A graphical comparison of the desired and attained modes is shown in Figure 27.

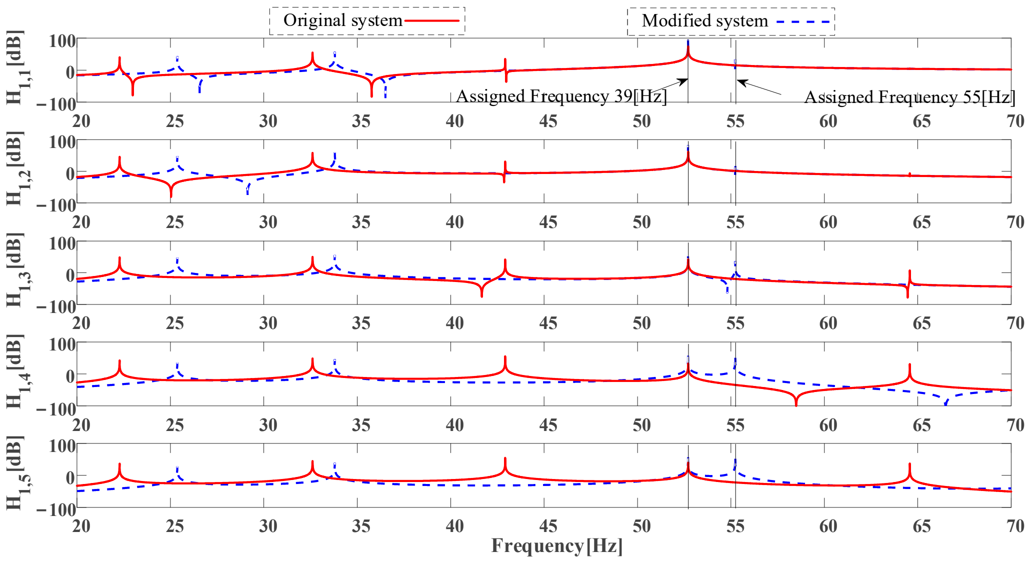

Figure 26. Original FRFs and the ones after adding supporting stiffness.

Table 18. Comparison of natural frequencies and mode shapes.

Frequency and Mode		Obtained	Frequency and Mode		Desired
f_i [Hz]	52.70	55.23	f_d [Hz]	39	55
u_i (1)	1.00	−0.060	u_d (1)	1.00	0
u_i (2)	−0.234	0.029	u_d (2)	−0.55	0.01
u_i (3)	0.021	−0.096	u_d (3)	0.2	−0.10
u_i (4)	0.044	0.883	u_d (4)	0	0.8
u_i (5)	0.041	1.000	u_d (5)	0.05	1.00
Desired mode number, d		1		2	
$\lvert f_d - f_i \rvert (100 \times \lvert f_d - f_i \rvert / f_d)$		13.7 (35.13)		0.23 (0.42)	
cos (u_d, u_i)		0.9511		0.9977	

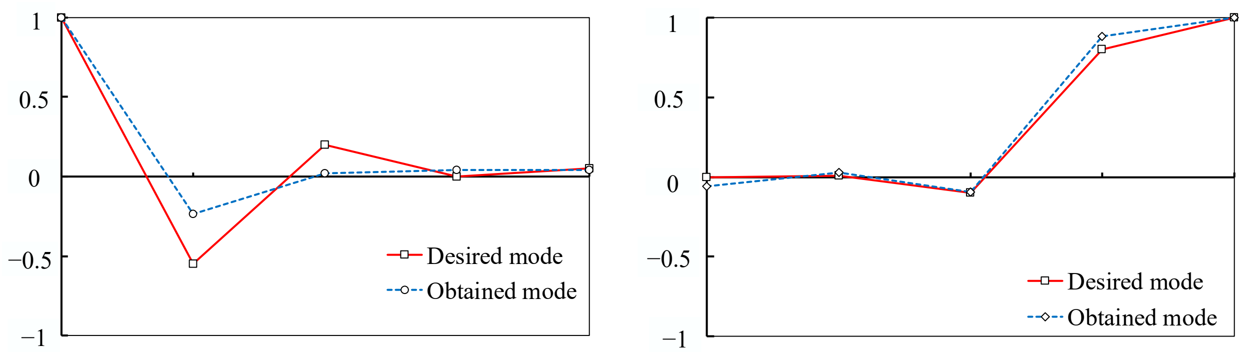

(a) **(b)**

Figure 27. Comparison of desired and attained modes: (**a**) 39 Hz; (**b**) 55 Hz.

The results shown in Table 18 demonstrate that the proposed method performed well in the assignment of frequency 55.00 Hz and the two desired modes, although the attained frequency of 52.7 Hz was far from the desired 39 Hz. This was due to fact that the number of desired modal parameters (two frequencies and ten mode elements) was much greater than that of modified variables (five added stiffness).

3.2.3. Simultaneous Addition of Masses and Stiffness

It was assumed that masses dm_1, dm_2, dm_3, dm_4, dm_5 and supporting stiffness dk_{11}, dk_{22}, dk_{33}, dk_{44}, dk_{55} were simultaneously added to the original system, as shown in Figure 18. The goal of this modification was to assign the two vibration modes listed in Table 3. The ranges of the added masses and stiffness were 0~2 kg and 0~300 kN/m, respectively. By solving the optimization Equation (24) using the genetic algorithm, the optimized values of added masses, the stiffness and the minimized values were obtained, as listed in Table 19:

Table 19. Parameters of added mass and stiffness.

Mass (kg)	Range	Value	Stiffness (kN/m)	Range	Value
dm_1	0–2	1.896	dk_{11}	0–300	4.230
dm_2	0–2	1.459	dk_{22}	0–300	12.931
dm_3	0–2	1.862	dk_{33}	0–300	36.959
dm_4	0–2	0.361	dk_{44}	0–300	192.893
dm_5	0–2	0.352	dk_{55}	0–300	85.339
minimized value			0.028191366967777782071		

The absolute values of the receptance $H_{1,i}$ (ω) (i = 1, ... , 5) of the original system (solid line) and the modified systems by the proposed method (dotted line) are shown in Figure 28. The natural frequencies and the modes obtained from the modified system are collected in Table 20. The difference between the cosine of the desired modes and the cosine of the attained modes is given in the last law of Table 20. A graphical comparison of the desired and attained modes is shown in Figure 29.

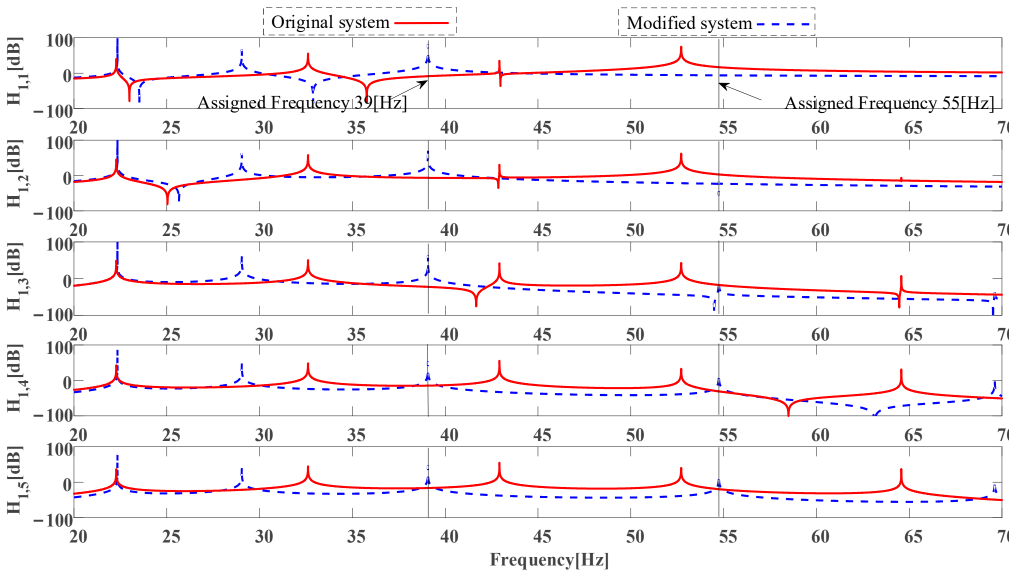

Figure 28. Original FRFs and FRFs after the simultaneous addition of masses and supporting stiffness.

Table 20. Comparison of natural frequencies and mode shapes.

Frequency and Mode		Obtained	Frequency and Mode		Desired
f_i [Hz]	39.07	54.74	f_d [Hz]	39	55
u_i (1)	1.00	−0.003	u_d (1)	1.00	0
u_i (2)	−0.568	0.089	u_d (2)	−0.55	0.01
u_i (3)	0.110	−0.066	u_d (3)	0.2	−0.10
u_i (4)	0.035	0.806	u_d (4)	0	0.8
u_i (5)	0.018	1.000	u_d (5)	0.05	1.00
Desired mode number, d		1		2	
$\lvert f_d - f_i \rvert$ ($100 \times \lvert f_d - f_i \rvert / f_d$)		0.07 (0.18)		0.26 (0.47)	
cos (u_d,u_i)		0.9960		0.9996	

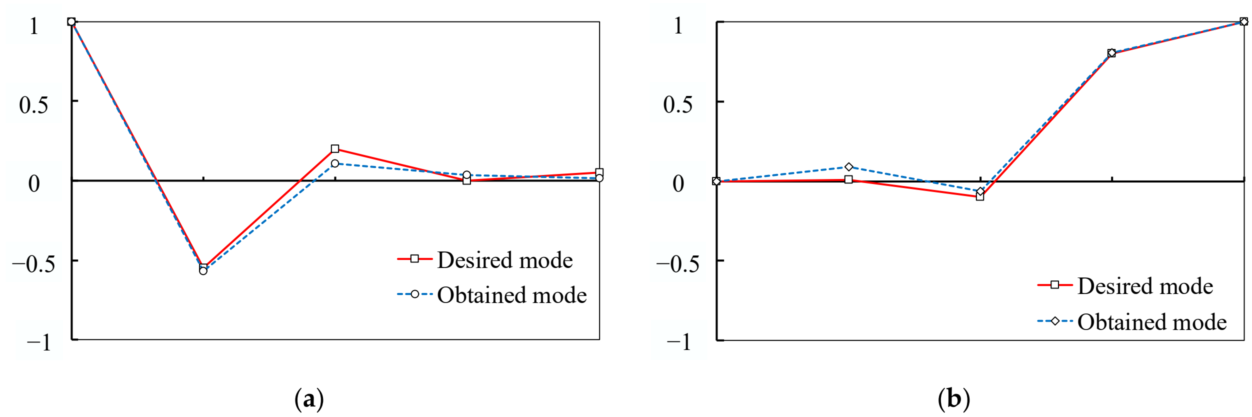

Figure 29. Comparison of desired and attained modes: (**a**) 39 Hz; (**b**) 55 Hz.

Compared with the addition of masses or supporting stiffness, the simultaneous addition of masses and stiffness clearly demonstrated better performances in both mode shapes and frequencies assignment. We believe that this was because the number of modifying quantities was increased from five (five added masses or five added stiffness) to ten (five added masses and five added stiffness).

3.2.4. Adding Spring-Mass Substructures

It was assumed that spring-mass substructures with masses dm_1, dm_2, dm_3, dm_4, dm_5 and stiffness dk_{11}, dk_{22}, dk_{33}, dk_{44}, dk_{55} were added to the original system, as shown in Figure 21. The goal of this modification was to assign the two vibration modes listed in Table 3. The ranges of the added masses and stiffness were 0~2 kg and 0~300 kN/m, respectively. By solving the optimization Equation (24) using the genetic algorithm, the optimized values of the substructures and the minimized values were solved and expressed in Table 21:

Table 21. Parameters of added masses and stiffness of substructures.

Mass (kg)	Range	Value	Stiffness (kN/m)	Range	Value
dm_1	0–2	1.036	dk_{11}	0–300	144.317
dm_2	0–2	0.891	dk_{22}	0–300	176.605
dm_3	0–2	0.809	dk_{33}	0–300	272.801
dm_4	0–2	0.986	dk_{44}	0–300	65.742
dm_5	0–2	1.012	dk_{55}	0–300	33.282
minimized value			0.027636992152442294		

The absolute values of the receptance $H_{1,i}$ (ω) (i = 1, . . . ,5) of the original system (solid line) and the modified systems by the proposed method (dotted line) are shown in Figure 30. The natural frequencies and the mode shapes obtained from the modified system are collected in Table 22. The difference between the cosine of the desired modes and the cosine of the attained modes is given in the last law of Table 22. A graphical comparison of the desired and attained modes is shown in Figure 31.

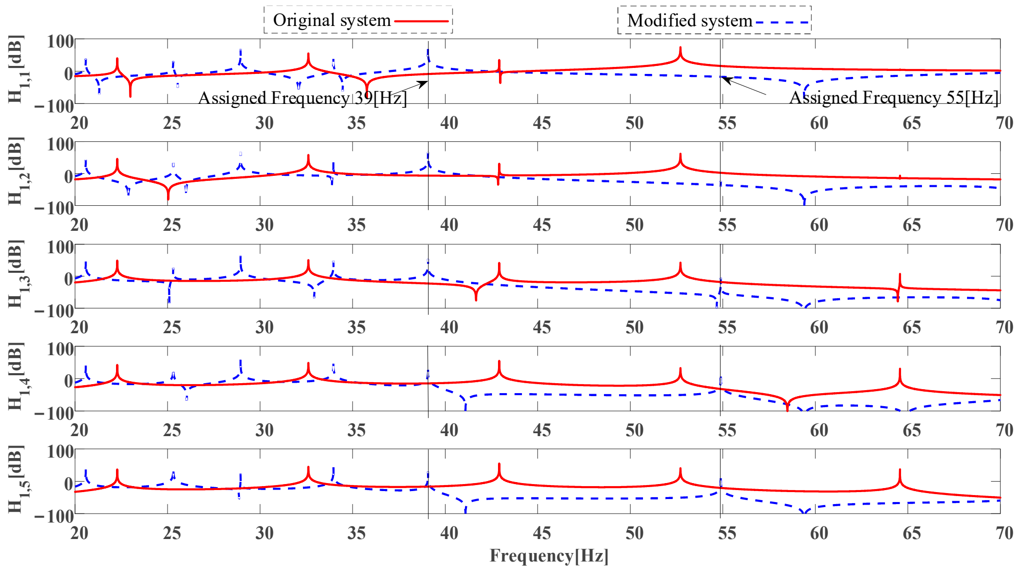

Figure 30. Original FRFs and FRFs after the addition of mass-spring substructures.

Table 22. Comparison of natural frequencies and mode shapes.

Frequency and Mode		Obtained	Frequency and Mode		Desired
f_i [Hz]	39.07	54.89	f_d [Hz]	39	55
u_i (1)	1.00	−0.001	u_d (1)	1.00	0
u_i (2)	−0.568	0.008	u_d (2)	−0.55	0.01
u_i (3)	0.127	−0.069	u_d (3)	0.2	−0.10
u_i (4)	−0.170	0.823	u_d (4)	0	0.8
u_i (5)	−0.008	1.000	u_d (5)	0.05	1.00
Desired mode number, d		1		2	
$\lvert f_d - f_i \rvert (100 \times \lvert f_d - f_i \rvert / f_d)$		0.07 (0.18)		0.11 (0.20)	
cos (u_d, u_i)		0.9966		0.9996	

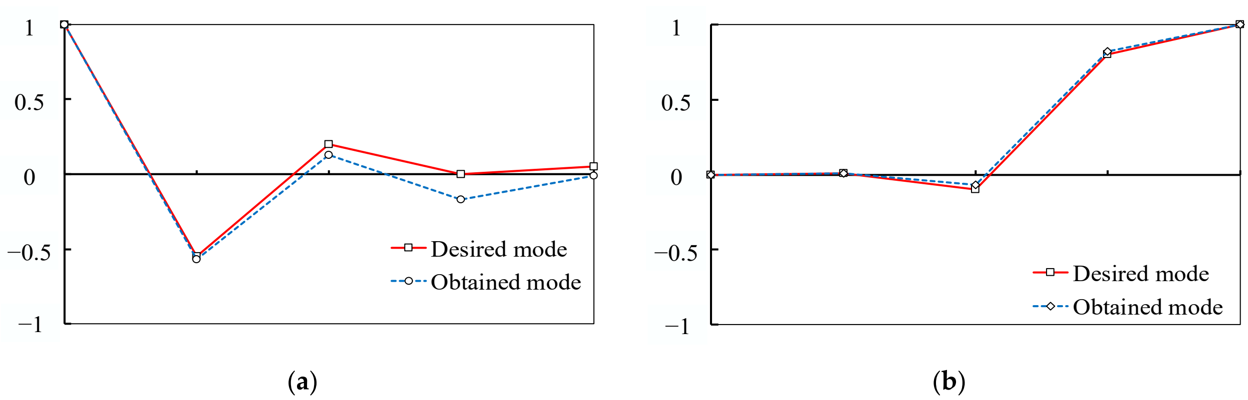

Figure 31. Comparison of desired and attained modes: (**a**) 39 Hz; (**b**) 55 Hz.

As with the simultaneous addition of masses and supporting stiffness, the addition of spring-mass substructures also demonstrated excellent performances in both mode shapes and frequencies assignment. This was also because more modification variables (five added masses and five added stiffness) were provided in the addition of substructures.

3.3. Discussion

It is evident that the proposed methods in Sections 3.1.1–3.1.4 demonstrated very good performances in the assignment of one natural frequency and mode shape. It can be seen from the results of the assignment of the natural frequencies and mode shapes in the above four structural modification schemes that the maximum error between the desired frequency and the attained frequency did not exceed 1.02% (when adding supporting stiffness), and that the smallest difference between the cosine of the desired mode and that of the attained mode was no less than 0.9431 (when adding masses). On the whole, the assigned natural frequencies and mode shapes of the modified system agreed well with the desired ones in all the four structural modification schemes. This indicates that when one natural frequency and mode need to be assigned, any of the above structural modification schemes can be chosen under the premise of convenient implementation in practice.

As can be seen in Sections 3.2.1–3.2.4, only partial frequencies and mode shapes were assigned by the structural modification of adding masses or stiffness when two frequencies and mode shapes needed to be assigned. However, all the frequencies and mode shapes were well assigned through the simultenous addition of masses and stiffness, or by adding a mass-spring subsystem. One reason for this phenomenon was that the latter structural modifications provided more modification variables, which made the optimization model more likely to obtain better results. Another reason lay in a law of structural dynamic modification, namely that the mere addition of masses will only lower the natural frequencies of the original structure, while the mere addition of stiffness will only heighten them. It is difficult to satisfy the assignment of multiple frequencies with these two kinds of unidirectional movement; the assignment of mode shapes should also be taken into consideration, which makes it even more difficult to meet the requirement of assigning multiple frequencies and mode shapes at the same time. By contrast, the addition of masses and stiffness simultaneously and the addition of mass-spring substructures both offer the possibility of lowering and heightening the natural frequencies of the original structure, making it easier to obtain better results when multiple frequencies and mode shapes need to be assigned at the same time. Based on the analysis above, we suggest that the addition of masses or stiffness should be considered for the sake of convenience in practical structural modification if fewer frequencies and mode shapes need to be assigned. We further suggest that either the simultaneous addition of masses and stiffness or the addition of mass-spring substructures can be chosen when multiple frequencies and mode shapes need to be assigned.

Compared with other assignment methods, the advantage of this method is that it can be applied to a variety of different structural modifications (the addition of masses, supporting stiffness, connection stiffness, and substructures, or the addition of a mixture of these), making this method more applicable to engineering. Furthermore, both frequencies and mode shapes were taken into consideration in the assignment; therefore, multiple frequencies and mode shapes can be assigned according to the proposed method. However, it is important to note that, as the number of frequencies and mode shapes that need to be assigned increases, it becomes more difficult to obtain better optimization results. Another merit of this FRFs-based method is that FRFs can be directly measured by modal testing, without knowledge of analytical or modal models. However, the influence of damping was not considered in this study in view of the fact that it damping relatively small in most engineering structures. For some cases, where the damping is relatively large, further analysis is required.

4. Conclusions

This study deals with the problem of frequencies and mode shapes assignment based on FRFs. Different structural modification schemes are considered in the method proposed in this study, including the addition of masses or stiffness (supporting stiffness or connection stiffness), the simultaneous addition masses and stiffness, and the addition of mass-spring substructures to the original structure.

A 5-DOF spring-mass vibration system was used in order to verify the accuracy and effectiveness of the proposed method. Both single frequency (and mode shape) and multiple natural frequencies (and mode shapes) assignments were validated. The results show that ideal results can be obtained by using any of the above-mentioned modification schemes when only one frequency and mode need to be assigned. However, it is difficult to assign multiple frequencies and mode shapes at the same time just by adding masses or stiffness. Correspondingly, either the simultaneous addition of masses and stiffness or the addition of a mass-spring subsystem are more likely to achieve better results when multiple frequencies and mode shapes are required. The main advantage of this method is that it can be applied to a variety of different structural modifications, making it more applicable to engineering. Another merit of this FRFs-based method is that FRFs can be directly measured by modal testing, without knowledge of analytical or modal models. This method is mainly applicable for the assignment of the natural frequencies and mode shapes of a structure with little damping in engineering.

Author Contributions: J.R. is the designer and executor of this study. J.R. and Q.C. completed the data analysis, wrote the paper, and revised it. All authors have read and agreed to the published version of the manuscript.

Funding: This research was funded by the Key Project of the Scientific Research Plan of the Hubei Provincial Department of Education, grant number D20211401.

Institutional Review Board Statement: Not applicable.

Informed Consent Statement: Not applicable.

Data Availability Statement: The data used to support the findings of this study are available upon request.

Conflicts of Interest: The authors declare no conflict of interest.

References

1. Ren, J.; Zhang, Q. Structural reanalysis based on FRFs using sherman–morrison–woodbury formula. *Shock Vib.* **2020**, *2020*, 1–12. [CrossRef]
2. He, J.; Li, Y. Relocation of anti-resonances of a vibratory system by local structural changes. *Int. J. Anal. Exp. Modal Anal.* **1995**, *10*, 224–235.
3. Joseph, K. Inverse eigenvalue problem in structural design. *AIAA J.* **1992**, *58*, 233–237. [CrossRef]
4. Ram, Y.; Braun, S. An inverse problem associated with modification of incomplete dynamic systems. *J. Appl. Mech.* **1991**, *58*, 223–237. [CrossRef]
5. Tsuei, Y.; Yee, E.K. A method for modifying dynamic properties of undamped mechanical systems. *J. Dyn. Syst. Meas. Control.* **1989**, *111*, 403–408. [CrossRef]
6. Liu, H. Eigenstructure Assignment in Vibration System. Ph.D. Thesis, Nanjing University of Aeronautics and Astronautics, Nanjing, China, 2007.
7. Belotti, R.; Ouyang, H.; Richiedei, D. A new method of passive modifications for partial frequency assignment of general structures. *Mech. Syst. Signal. Pr.* **2018**, *99*, 586–599. [CrossRef]
8. Syrmos, V.L.; Lewis, F.L. Robust eigenvalue assignment for generalized systems. *Automatica* **1992**, *28*, 1223–1228. [CrossRef]
9. Kautsky, J.; Nichols, N.K. Algorithms for Robust Pole Assignment in Singular Systems. In Proceedings of the 1986 American Control Conference, Seattle, WA, USA, 18–20 June 1986.
10. Cobb, R.G.; Liebst, B.S. Structural damage identification using assigned partial eigenstructure. *AIAA J.* **1997**, *35*, 152–158. [CrossRef]
11. Duan, G. Eigenstructure assignment and response analysis in descriptor linear systems with state feedback control. *Int. J. Control.* **1998**, *69*, 663–694. [CrossRef]
12. Duan, G.; Patton, R.J. Eigenstructure assignment in descriptor systems via state feedback: A new complete parametric approach. *Int. J. Syst. Sci.* **1998**, *29*, 167–178. [CrossRef]
13. Duan, G.R. Solution to matrix equation AV + BW = EVF and eigenstructure assignment for descriptor systems. *Automatica* **1992**, *28*, 639–642. [CrossRef]

14. Fahmy, M.M.; O'Reilly, J. Parametric eigenstructure assignment for continuous-time descriptor systems. *Int. J. Control.* **1989**, *49*, 129–143. [CrossRef]
15. Fletcher, L.; Kautsky, J.; Nichols, N. Eigenstructure assignment in descriptor systems. *IEEE. T. Automat. Contr.* **1986**, *31*, 1138–1141. [CrossRef]
16. Duan, G. Eigenstructure assignment in descriptor systems via output feedback: A new complete parametric approach. *Int. J. Control.* **1999**, *72*, 345–364. [CrossRef]
17. Fletcher, L. Eigenstructure assignment by output feedback in descriptor systems. *IEE Proc.-D.* **1988**, *135*, 302–308. [CrossRef]
18. Duan, G.; Patton, R.J. Robust pole assignment in descriptor systems via proportional plus partial derivative state feedback. *Int. J. Control.* **1999**, *72*, 1193–1203. [CrossRef]
19. Kyprianou, A.; Mottershead, J.E.; Ouyang, H. Assignment of natural frequencies by an added mass and one or more springs. *Mech. Syst. Signal. Pr.* **2004**, *18*, 263–289. [CrossRef]
20. Mottershead, J.E.; Tehrani, M.G.; Ram, Y.M. Eigenvalue assignment problems in vibration using measured receptances: Passive Modification and active control. In *Dynamical Inverse Problems: Theory and Application*; Gladwell, G.M.L., Morassi, A., Eds.; Springer Vienna: Vienna, Austria, 2011; pp. 179–202.
21. Ouyang, H.; Richiedei, D.; Trevisani, A.; Zanardo, G. Eigenstructure assignment in undamped vibrating systems: A convex-constrained modification method based on receptances. *Mech. Syst. Signal. Pr.* **2012**, *27*, 397–409. [CrossRef]
22. Mao, X.; Dai, H. Minimum norm partial eigenvalue assignment of high order linear system with no spill-over. *Linear Algebra Appl.* **2013**, *438*, 2136–2154. [CrossRef]
23. Hu, Z.; Zhang, J.; Yang, H.; Wang, G.; Singh, K.V. A new approach for symmetry preserving partial eigenstructure assignment of undamped vibrating systems. *Shock Vib.* **2015**, *2015*, 629109. [CrossRef]
24. Ouyang, H.; Zhang, J. Passive modifications for partial assignment of natural frequencies of mass—Spring systems. *Mech. Syst. Signal. Pr.* **2015**, *50*, 214–226. [CrossRef]
25. Liu, Z.H.; Li, W.Y.; Ouyang, H.; Wang, D.H. Eigenstructure assignment in vibrating systems based on receptances. *Arch. Appl. Mech.* **2015**, *85*, 713–724. [CrossRef]
26. Belotti, R.; Richiedei, D.; Trevisani, A. Optimal design of vibrating systems through partial eigenstructure assignment. *J. Mech. Design.* **2016**, *138*, 071402. [CrossRef]
27. Bai, Z.; Wan, Q. Partial quadratic eigenvalue assignment in vibrating structures using receptances and system matrices. *Mech. Syst. Signal. Pr.* **2017**, *88*, 290–301. [CrossRef]
28. Cakar, O. A method for shifting natural frequencies of a dynamic system to desired values with concentrated mass modifications. *J. Vibroeng.* **2018**, *20*, 1–12. [CrossRef]
29. Belotti, R.; Richiedei, D. Dynamic structural modification of vibrating systems oriented to eigenstructure assignment through active control: A con-current approach. *J. Sound Vib.* **2018**, *422*, 358–372. [CrossRef]
30. Tsai, S.; Ouyang, H.; Chang, J. A receptance-based method for frequency assignment via coupling of subsystems. *Arch. Appl. Mech.* **2020**, *90*, 449–465. [CrossRef]
31. Çakar, O. Mass and stiffness modifications without changing any specified natural frequency of a structure. *J. Vib. Control.* **2010**, *17*, 769–776. [CrossRef]